Journal of Cerebral Blood Flow & Metabolism (2014) 34, 307–315

www.jcbfm.com

ORIGINAL ARTICLE

Sterile inflammation after permanent distal MCA occlusion in hypertensive rats

Karoline Möller[1,2], Johannes Boltze[1,3,4], Claudia Pösel[1], Johannes Seeger[2], Tobias Stahl[5,6] and Daniel-Christoph Wagner[1,3,6]

The pathophysiology of stroke is governed by immune reactions within and remote from the injured brain. Hypertension, a major cause and comorbidity of stroke, entails systemic vascular inflammation and may influence poststroke immune responses. This aspect is, however, underestimated in previous studies. Here we aimed to delineate the sequence of cellular inflammation after stroke in spontaneously hypertensive (SH) rats. Spontaneously hypertensive rats were subjected to permanent middle cerebral artery occlusion and killed after 1 or 4 days. Immune cells of the peripheral blood and those which have infiltrated the injured brain were identified and quantified by flow cytometry. The spatial distribution of myeloid cells and T lymphocytes, and the infarct volume were assessed by histology. We observed a concerted infiltration of immune cells into the ischemic brain of SH rats. At day 1, primarily neutrophils, monocytes, macrophages, and myeloid dendritic cells entered the brain, whereas the situation at day 4 was dominated by microglia, macrophages, lymphatic dendritic cells, and T cells. Postischemic inflammation did not cause secondary tissue damage during the subacute stage of experimental stroke in SH rats. Considering the intrinsic vascular pathology of SH rats, our study validates this strain for further translational research in poststroke inflammation.

Journal of Cerebral Blood Flow & Metabolism (2014) **34,** 307–315; doi:10.1038/jcbfm.2013.199; published online 13 November 2013

Keywords: cerebral ischemia; flow cytometry; inflammation; microglia; spontaneously hypertensive rat

INTRODUCTION

Sterile inflammation significantly influences the pathophysiological course of ischemic stroke. A concerted cascade of innate and adaptive immune reactions starts immediately after the disruption of cerebral blood flow and is characterized by successive waves of leukocyte subsets infiltrating the injured brain.[1] These processes have been considered to mediate both beneficial and adverse effects on disease progression during the acute and subacute stages of stroke.[2–4] Consequently, the modulation of postischemic inflammation represents an eligible approach toward novel treatment strategies.[5] However, translational research in this field is complicated by the fact that the rodent immune system including its specific responses is only partially comparable with the human one.[6] This obstacle could at best be met by the use of different strains and species to ultimately improve the prognostic power of preclinical findings.[7] The predictability of preclinical experiments might be further shortened by the predominant use of young and healthy animals, even though stroke patients usually experience relevant comorbidities such as arterial hypertension and chronic systemic inflammation due to hypertensive vascular damage.[8] In fact, hypertension and cerebral small vessel disease (SVD) as one of its important sequelae are among the major causes for stroke and significantly worsen its outcome.[9] However, although highly relevant for stroke patients, little is known about the mutual interaction of vascular inflammation caused by hypertension[10] and postischemic sterile inflammation.

Spontaneously hypertensive (SH) rats have been used for decades to study arterial hypertension. Interestingly, there is growing evidence that SH rats and hypertensive human patients share common pathophysiological characteristics of neurogenic hypertension including vascular inflammation and cerebral microvessel alterations, which are pathognomonic for SVD.[10–12] Recent clinical and preclinical investigations revealed that hypertension activates a plethora of inflammatory cascades including chronic activation of microglia,[12] thereby constituting a specific prerequisite for the immunologic facet of cerebral stroke. We hence considered SH rats to be a promising animal model for studying postischemic inflammation and immunodepression closely correlated to pathophysiological conditions existing in human stroke patients. Here we report on postischemic inflammation in SH rats at day 1 and 4 after permanent middle cerebral artery occlusion. Brain infiltrating and peripheral blood immune cells were identified and quantified by means of multidimensional flow cytometry. The influence of the stroke model was controlled by time-matched sham control groups.

MATERIALS AND METHODS

Animals and Experimental Stroke

Animal experiments were approved by the local animal welfare committee (Landesdirektion Sachsen, license number TVV 18/07) and conducted according to the Guide for the Care and Use of Laboratory Animals published by the US National Institutes of Health (NIH Publication No. 85-23, revised 1996). Altogether 40 male SH rats at the age of 12 to 14 weeks (Charles River, Sulzfeld, Germany) were housed in groups of five with free access to food and water. The subjects were kept under conditions of constant temperature and humidity and were further exposed to an artificial light–dark cycle. Animals were randomly assigned to one of the following experimental groups: (i) flow cytometry at day 1 and 4 after

[1]Fraunhofer Institute for Cell Therapy and Immunology, Leipzig, Germany; [2]Institute of Veterinary Anatomy, University of Leipzig, Leipzig, Germany; [3]Translational Centre for Regenerative Medicine, University of Leipzig, Leipzig, Germany; [4]Massachusetts General Hospital and Harvard Medical School, Boston, Massachusetts, USA and [5]IDT Biologika GmbH, Dessau-Rosslau, Germany. Correspondence: K Möller, Fraunhofer Institute for Cell Therapy and Immunology, Perlickstrasse 1 04103 Leipzig, Germany.
E-mail: karoline.moeller@izi.fraunhofer.de
[6]These authors contributed equally to this work.
Received 16 May 2013; revised 18 October 2013; accepted 21 October 2013; published online 13 November 2013

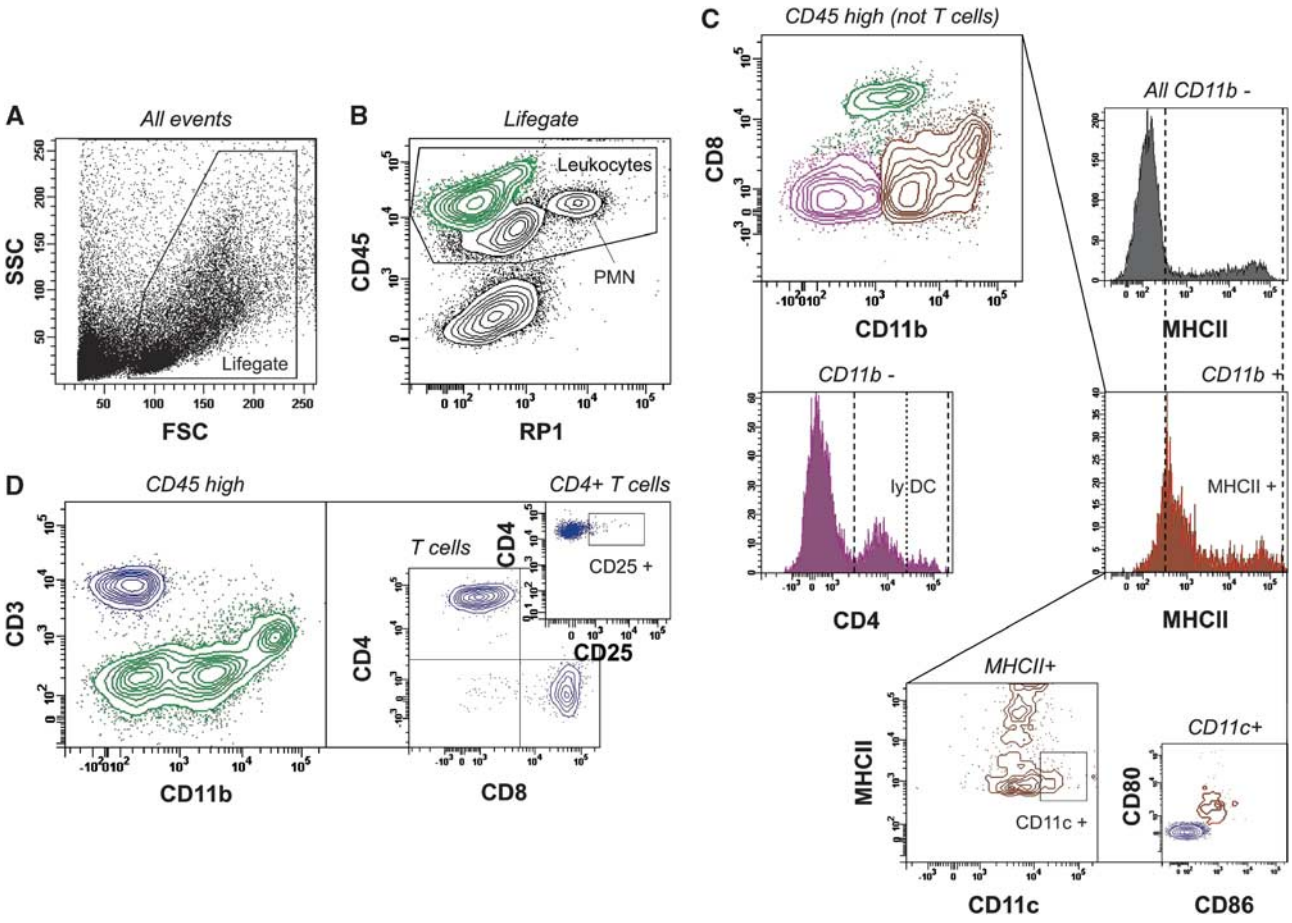

Figure 1. Gating strategy for the analysis of resident and brain-infiltrating leukocytes. Initially, viable leukocytes were detected based on morphologic parameters (**A**) and CD45 expression (**B**). CD45 intermediate (int) neutrophils were characterized by RP1 expression (**B**, PMN), and by being CD45 int/CD11b + /CD80 − /CD86 − /MHCII − . Microglia was identified by a CD45 low/RP1 − profile (**B**) and further denoted as CD11b + /CD3 − /CD8 − /CD4 ± cells. Total CD45 high cells (**B**, green) were further discriminated (**C**, **D**). CD3 − /CD11b int/CD8 + events were classified as natural killer cells (C, green, for additional confirmation of their identity refer to Supplementary Figure 1). CD3 − /CD11b − /CD8 − cells (**C**, purple) could be divided into a CD4 − and a CD4 + type (**C**, purple histogram), at which the CD4 + subtype was considered as lymphoid dendritic cells (lyDC). CD11b + cells (**C**, ocher) were classified as myeloid cells composed of monocytes, macrophages, and dendritic cells (DC). These cells were further discriminated into MHCII − monocytes and MHCII + macrophages/DC (ocher histogram, plus depiction of total CD11b − cells in the gray histogram). The latter population could be further distinguished into MHCII int/CD11c + /CD80 + /CD86 + myeloid DC (**C**, medium and small plot, including comparative display of T lymphocytes). T cells were identified being CD3 + /CD11b − (**D**, blue) and subsequently discriminated into CD8 + cytotoxic T cells, CD4 + T helper cells and few CD8 − /CD4 − cells (**D**, medium plot). A further small T-cell subpopulation was classified by CD4 and CD25 expression (**D**, small plot). FSC, forward light scatter; SSC, side light scatter.

either stroke or sham surgery ($n = 30$); (ii) histology at day 1 and 4 after stroke ($n = 10$). Groups (i) also contained naïve animals without any surgical intervention. Permanent right middle cerebral artery occlusion was induced in male SH rats at the age of 12 to 14 weeks as described previously.[13] Briefly, the right temporal bone and dura mater were opened, and the subjacent middle cerebral artery was permanently occluded by thermocoagulation. Sham surgery was performed by conducting the identical surgical procedure including the pre- and postoperative treatment, but omitting the thermo-occlusion of the artery. During anesthesia, the body temperature was monitored and maintained at 37.5°C using a feedback-regulated heating pad. Postoperative analgesia was provided for 3 days by Metamizole (Ratiopharm, Ulm, Germany) dissolved in sweetened drinking water (100 mg in 40 mL). Functional deficits were assessed at day 1 and 4 using the modified neurologic severity score as described previously.[14] No animal died during surgery or prematurely throughout the experiment.

Tissue Sampling

At allocated time points, subjects were deeply anesthetized with ketamine hydrochloride (100 mg/kg) and xylazine (10 mg/kg) and then killed by CO_2 exposition. The thoracic cavity was opened, the left ventricle was punctured, and 1 mL samples of peripheral blood were collected. Animals were immediately perfused transcardially with 200 mL of cold phosphate-buffered saline. For flow cytometry (group i) brains were removed, dissected, and stored in Hanks Balanced Salt Solution on ice for 30 minutes. Spleens were harvested and weighed. For histologic analyses (group ii) animals were additionally perfused with 200 mL ice-cold formalin solution (4%). Removed brains were postfixed overnight in formalin solution, cryopreserved by sucrose infiltration (30%) up to saturation, and finally cooled down to −80°C. Frozen brains were cut in 20 μm thick coronal cryosections and mounted on coated slides for subsequent immunofluorescence and hematoxylin and eosin staining procedures.

Processing of Peripheral Blood

Blood cell counts were determined using an Animal Blood Counter (ABL, Vet scil animal care company, Viernheim, Germany). Heparinized blood samples were aliquoted to 50 μL, diluted with 50 μL phosphate-buffered saline and 10 μL normal mouse serum and preincubated for 30 minutes at room temperature. Samples were stained with the following mouse–anti-rat antibodies: CD3-FITC, CD8-PerCP, CD4-PECy7, CD11b-PacificBlue (Supplementary Table 1). After incubation for 20 minutes at 4°C, all samples were subjected to hypotonic erythrolysis in distilled water for

30 seconds followed by repeated washing steps in phosphate-buffered saline containing 3% fetal calf serum. Cells were then resuspended in 300 μL buffer and immediately subjected to acquisition.

Processing of Brain Tissue

Leukocytes were isolated from the right hemispheres (with the ischemic lesion in MCAO subjects) as described previously.[15] Briefly, the cerebellum and the olfactory bulb were removed and the remaining brain tissue was mechanically dissected in Hanks Balanced Salt Solution. Suspensions were further processed by intermittent enzymatic digestion with collagenase I (Sigma, Munich, Germany) and DNAse I (Roche, Mannheim, Germany) for 45 minutes at 37°C, including two trituration steps. The resulting cell suspensions were separated by density gradient centrifugation on discontinuous Percoll (GE Healthcare, München, Germany) gradients composed of four sequent layers (80%/38%/21% Percoll covered with cell culture medium). Cells accumulating in between 80%/38% Percoll were harvested and washed repeatedly. Viable cells per hemisphere were counted using trypan blue exclusion. Aliquots of 10E5 cells were resuspended in 100 μL FACS buffer (phosphate-buffered saline containing 3% fetal calf serum), preincubated with 10% normal mouse serum and specific FC-blocking reagent (purified anti-rat CD32) at 4°C for 20 minutes before being labeled with multiple combinations of the following anti-rat antibodies: CD3-FITC, MHCII-AlexaFluor488, anti-granulocytes-PE (RP1), CD86-PE, CD45-PECy5, CD8-PerCP, CD4-PECy7, CD11c-purified, CD25-biotin, CD80-biotin, CD11b-PacificBlue (Supplementary Table 2). Primary antibody incubation was performed for 20 minutes at 4°C in the dark followed by multiple blocking and washing steps and secondary labeling if applicable (Supplementary Table 3). Cells were then resuspended in 300 μL FACS buffer and stored at 4°C in the dark until acquisition.

Flow Cytometric Acquisition and Analysis

Acquisition and analysis were performed using a 3-laser FACSCanto II equipped with the FACSDiva software (BD Biosciences, Heidelberg, Germany) by an investigator masked to the group allocation. Specific cell subpopulations were identified by their antigen expression. An exemplary gating scheme and the denomination of major brain cell populations identified in this study are displayed in Figure 1. Absolute cell numbers were calculated by multiplication of total viable cell counts per hemisphere (brain) or total white blood counts (peripheral blood) by the percentage of the depicted subpopulations out of the viable cell gate (Lifegate).

Immunofluorescence Staining and Infarct Volumetry

For visualization of the myeloid cells and T cells, brain sections were blocked with 5% goat serum and 0.3% Trition X-100 for 30 minutes and incubated with either polyclonal rabbit anti-Iba1 (ionized calcium binding adaptor molecule 1; 1:200; Wako Chemicals, Neuss, Germany), biotinylated solanum tuberosum lectin (STL; 1:300; Linaris, Dossenheim, Germany), monoclonal mouse anti-15-16A1 (1:500; Hycult Biotech, Beutelsbach, Germany; for T cells) for 24 hours at 4°C. Sections were then incubated with goat anti-rabbit immunoglobulin G (1:200, Invitrogen, Darmstadt, Germany), goat anti-mouse immunoglobulin G (1:200, Invitrogen) or streptavidin (Dianova, Hamburg, Germany) conjugated with either Alexa Fluor 488, 546, or Cy5 for 1 hour at room temperature. All sections were counterstained with 4′,6-diamidino-2-phenylindole (2.5 μg/mL, Sigma). As negative controls, one brain section from each slide was processed analogously to the staining procedure omitting primary antibody incubation. Fluorescence images were acquired using a Zeiss (Göttingen, Germany) LSM710 confocal laser scanning microscope (Laser: Diode 405, Argon 488, HeNe 543; objective: Plan-Apochromat $\times$63/1.40 oil). For the spatial analysis of myeloid and T cells, stained sections from two different brain regions (bregma anteroposterior $+1.5$ mm and 1.0 mm) per animal (for five animals per time point) were inspected for distribution of neutrophils (STL+/Iba1−/segmented nucleus) monocytes (STL+/Iba1−/non-segmented nucleus), macrophages/microglia (STL+/Iba1+) and T cells (15 to 16A1+ cells). For determination of infarct volumes, 10 sequential coronal sections between bregma $+4.0$ mm and -5.0 mm were stained with hematoxylin and eosin and images were acquired using a Nikon Coolscan V ED scanner. Areas of the ischemic infarct, corpus callosum, striatum, and the remaining cortex were assessed on each section by using ImageJ (National Institutes of Health) software and summarized to the respective volumes.

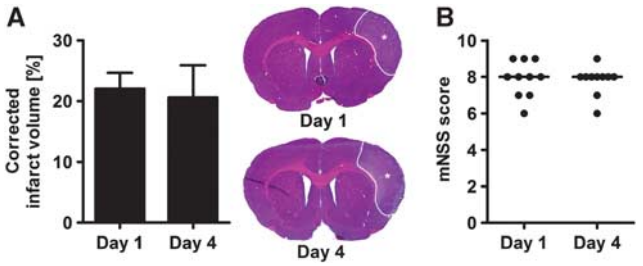

Figure 2. Ischemic lesion and functional deficit. (**A**) The edema-corrected infarct volume was determined on serial hematoxylin and eosin (H&E)-stained sections. The ischemic lesion could be demarcated as pale area within the supply territory of the right middle cerebral artery (tagged by asterisks). No significant differences were found between animals that survived 1 and 4 days ($P>0.05$ by *t*-test for $n=5$ animals per group). (**B**) The modified neurologic severity score (mNSS) revealed a constant functional deficit at day 1 and 4 after stroke ($P>0.05$ by Mann–Whitney test for $n=10$ animals per group; lines indicate the median values).

Statistical Analysis

Statistical differences were analyzed by *t*-test (infarct volume and volumetric analyses), Mann–Whitney rank sum test (modified neurologic severity scoring), or by one-way analysis of variance. Multiple *post hoc* testing was performed with Bonferroni's multiple comparison test. Thus, the MCAO groups (D1 and D4) were compared first with the corresponding sham controls, second to the naïve controls, and third to each other. Furthermore, the sham groups were compared with the naïve controls to control the impact of surgery. *P* values $\leqslant 0.05$ were considered statistically significant (*). Highly significant differences were indicated separately for $P\leq 0.01$ (**) or $P\leq 0.001$ (***). Data are given as mean $\pm$ s.d., or otherwise as stated.

RESULTS

Ischemic Lesion Development

We first investigated whether the postischemic cerebral inflammation is accompanied by a change of the ischemic lesion volume or by delayed tissue loss within the primarily uninvolved brain regions. We did not find a significant difference between the ischemic lesion volume at day 1 and 4 after stroke (Figure 2A). The volumetric analyses of the remaining cortical tissue (day 1: 151.0 ± 6.1 versus day 4: 148.5 ± 10.5 mm^3), striatum (day 1: 32.2 ± 2.8 versus day 4: 30.9 ± 2.7 mm^3) and corpus callosum (day 1: 17.9 ± 2.5 versus day 4: 19.8 ± 1.1 mm^3) revealed no significant difference between both time points ($P>0.05$ by *t* tests). We next evaluated the neurologic deficits after stroke by means of the modified neurologic severity score and found similarly increased score points at day 1 and 4 after stroke (Figure 2B).

Systemic Impact of Ischemic Stroke

In order to examine the influence of brain ischemia on the overall immune status in SH rats, blood samples were taken at days 1 and 4 and analyzed by means of automated blood cell counting and flow cytometry. Concurrently with the brain tissue sampling, spleens were removed and weighed. The absolute counts for white blood cells, red blood cells, platelets, hemoglobin, and hematocrit did not significantly differ among the experimental groups (Supplementary Table 4). However, the differentiation of leukocyte subpopulations by flow cytometry revealed a systemic effect of both surgical intervention and brain ischemia. First, we found an almost twofold increase of blood monocytes at the later time point after stroke that was, however, statistically not distinguishable from the time-matched sham control group (Figure 3A). Next, we observed a threefold increase of granulocyte counts at day 1 both in the sham group and more pronounced after experimental stroke (Figure 3B). At the later time point, we

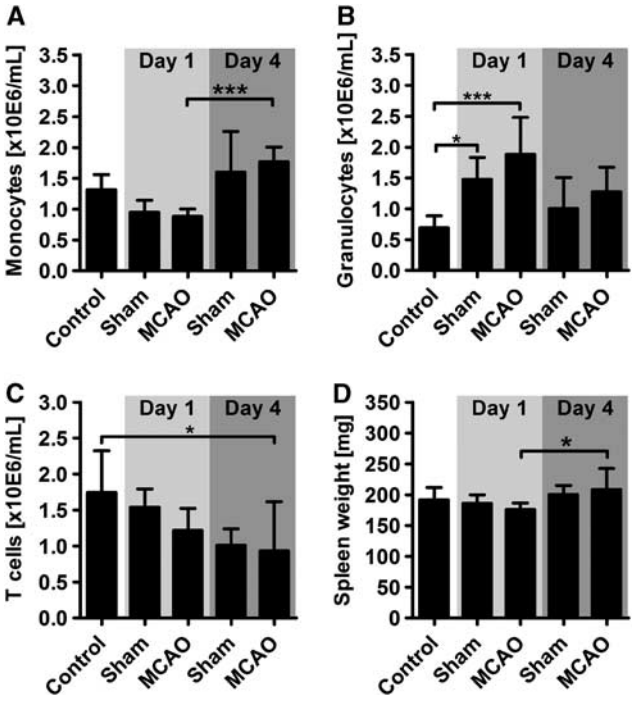

Figure 3. Peripheral blood leukocyte counts after stroke. (**A**) Monocytes significantly increased 4 days after middle cerebral artery occlusion (MCAO) compared with day 1, although no differences were acquired to the time-matched sham control or naïve control. (**B**) The absolute number of granulocytes showed a highly significant increase at day 1 after MCAO compared with the naïve control but not to the time-matched sham control. (**C**) Compared with naïve controls, significantly less T cells were detected in stroke animals after 4 days. (**D**) Spleen weights of ischemic animals at day 4 were significantly higher than at day 1 but without differences to either the sham or naïve control. Weights were normalized to total body mass. $^{*}P<0.05$; $^{***}P<0.001$ by one-way analysis of variance for $n=5$ to 7 animals per group.

found the granulocytosis normalized to control levels. T cell counts decreased at day 4 after stroke, only when compared with naïve controls but not to time-matched sham controls (Figure 3C). The distribution of T-cell subpopulations was found to be consistent among all experimental groups with a CD4/CD8 ration of 3:2. Natural killer cells did not vary significantly between the experimental groups (control: $0.6\pm0.2\times10$E6 cells per mL; sham D1: $0.6\pm0.2\times10$E6 cells per mL; MCAO D1: $0.5\pm0.1\times10$E6 cells per mL; sham D4: $0.7\pm0.4\times10$E6 cells per mL; MCAO D4: $0.7\pm0.4\times10$E6 cells per mL; $P>0.05$ by one-way analysis of variance). We found a significant increase of the spleen weight between day 1 and 4 after stroke (Figure 3D).

Myeloid Cells Sequentially Emerge in the Ischemic Brain

We next analyzed the inflammatory infiltrate within the ischemic brain and found a significant two- to threefold increase of CD45+ leukocytes at days 1 and 4 after stroke when compared with the appropriate control conditions (Figure 4A). The leukocytes were further classified into myeloid and non-myeloid cells by CD11b expression. Myeloid cells that accounted for the majority of leukocytes in all experimental groups were strongly elevated at day 1 and 4 after stroke (Figure 4A). The subdifferentiation of CD11b+ myeloid cells revealed that the infiltrate at day 1 was dominated by neutrophils (Figure 4B), monocytes (Figure 4C), and macrophages (Figure 4D) whereas microglia counts were comparable with control conditions (Figure 4E). However, at day 4 after the onset of stroke, both neutrophil and monocyte counts decreased toward control levels (Figures 4B and 4C). In contrast, macrophage numbers remained elevated (Figure 4D) and the amount of microglia cells increased by almost 300% thus constituting the major part of myeloid cells at day 4 (Figure 4E). Interestingly, we found both in naïve controls and at day 4 that more than 90% of the microglia expressed the CD4 receptor (Figure 4F), which is significantly increased compared with naïve normotensive animals (Supplementary Figure 2). At day 1 after stroke, the proportion of the residual CD4− microglia was significantly and transiently increased (Figure 4F).

Spatial Distribution of Myeloid Cells in the Ischemic Hemisphere

We next aimed to expand our quantitative data on myeloid cell infiltration by immunohistochemical visualization of neutrophils, monocytes, and macrophages/microglia using a triple fluorescence staining method. In the contralateral cortex, we exclusively found ramified microglia double positive for STL and Iba1 (Figure 5A). At day 1 after stroke, we observed a hypertrophy of microglia in the infarct border zone (Figure 5B) whereas the ischemic lesion was almost completely depleted from STL+/Iba1+ cells. Interestingly, at the same time point, we found numerous myeloid cells within the meninges and the subjacent ischemic tissue. Monocytes were mainly found in the ischemic cortical tissue, forming a band beneath the meninges (at the level of cortical layer III; Figure 5D). In contrast, both neutrophils and macrophages were primarily localized in the meninges and directly thereunder (Figure 5E). At day 4 after stroke, we found only few polymorphonuclear neutrophils throughout the ischemic hemisphere. In contrast, the ischemic lesion border was characterized by a plethora of STL+/Iba1+ cells. These cells exhibited a morphologic heterogeneity, ranging from ramified (toward unaffected brain tissue) to round (toward the ischemic lesion) phenotypes with several interstages (Figures 5F and 5G). Few Iba1− monocytes were detectable among the round STL+/Iba1+ cells within the lesion (Figure 5G). Surprisingly, the region of intensive infiltration at day 1 showed only minor numbers of round STL+/Iba1+ cells at day 4.

Time Course of Non-Myeloid Cell Infiltration into the Ischemic Brain

In contrast to the massive increase of myeloid cells after experimental stroke, the CD11b− cell population showed only slight differences at day 4 (Figure 5A). Whereas CD4+ T helper cell counting did not expose significant differences between ischemic and control animals, we observed significantly increased counts for CD8+ cytotoxic T cells at day 4 (Figures 6A and 6B). Furthermore, we differentiated two small T-cell subpopulations by either missing expression of CD4 and CD8 (double-negative T cells), or by co-expression of CD4 and the activation marker CD25. Both populations significantly increased 4 days after stroke, but not earlier (Figures 6C and 6D). To investigate the spatial distribution of T cells within the ischemic brain, we used immunohistochemical staining of the pan T-cell marker 15-16A1. One day after MCAO, we found scattered T cells within the ipsilateral and contralateral hemisphere without any site-specific accumulation. On the contrary, at day 4, we observed an increase of T cells throughout the entire ipsilateral hemisphere. In the cortical infarct border, and even more pronounced in the ischemic lesion, numerous T cells were found around blood vessels (Figures 6E and 6F). In the ischemic lesion, T cells were also found within the vessels (Figure 6G). Finally, numerous T cells were found among STL+ cells within in the meninges (Figure 6H). Next, we analyzed the dynamics of CD11b INT/CD8+ natural killer cells after cerebral ischemia and found this lymphocyte population to be surprisingly numerous in the naïve SH rat brain ($28.5\pm16.1\times10$E3 cells, amounting for $\sim$ 25% of all leukocytes). However, the absolute natural killer cell numbers remained unaltered after

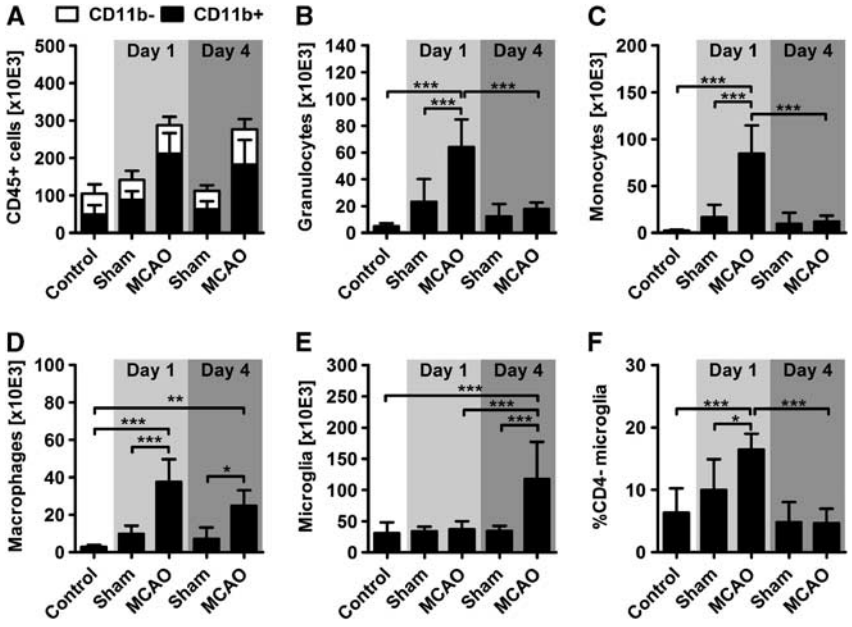

Figure 4. Characterization of brain-infiltrating myeloid cells after stroke. (**A**) CD45+ leukocytes (black plus white bars) were augmented in ischemic brains at day 1 and 4 after stroke ($P<0.001$ versus time-matched sham controls and healthy control). At day 1, this increase was exclusively driven by CD11b+ myeloid cells (black bars; $P<0.001$ versus sham and naïve control), whereas at day 4 both CD11b+ cells and CD11b- cells (white bars) were increased compared with sham conditions ($P<0.05$). At day 1 after stroke, it was evident that substantial numbers of granulocytes (**B**), monocytes (**C**), and macrophages (**D**) entered the ischemic hemisphere. Statistical significance was found in each case in comparison with both the time-matched sham and naïve controls. Cell counts of granulocytes and monocytes were found to be normalized at day 4, whereas macrophage counts remained elevated (**D**) and microglia cells significantly increased (**E**). The amount of CD4-expressing microglia transiently increased at day 1 after stroke (**F**). *$P<0.05$; **$P<0.01$; ***$P<0.001$ by one-way analysis of variance for $n=5$ to 8 animals per group. MCAO, middle cerebral artery occlusion.

stroke (sham D1: $20.1\pm13.7\times10E3$ cells; MCAO D1: $26.6\pm14.4\times10E3$ cells; sham D4: $18.9\pm7.6\times10E3$ cells; MCAO D4: $31.6\pm17.0\times10E3$ cells; $P>0.05$ by one-way analysis of variance). The residual CD11b−/CD8−/CD4− population was not further differentiated in this study, but contains ~60% CD45RA+ B cells and other non-myeloid cells (Supplementary Figure 1B). This population significantly increased both at day 1 and 4 after stroke when compared with the controls (control: $12.2\pm4.9\times10E3$ cells; sham D1: $13.0\pm5.1\times10E3$ cells; MCAO D1: $24.9\pm8.9\times10E3$ cells; sham D4: $12.1\pm3.7\times10E3$ cells; MCAO D4: $23.2\pm7.7\times10E3$ cells; $P<0.001$ by one-way analysis of variance).

Differentiation of Dendritic Cells among the Brain Infiltrate

In a final step, we differentiated two putative dendritic cell populations that participate in the inflammatory response to stroke. First, we observed a CD11b+/CD11c+ myeloid dendritic cell population that transiently increased at day 1 after MCAO (Figure 7A). Second, we detected CD4+ lymphoid dendritic cells that increased from day 1 to day 4 after stroke (Figure 7B). Notably, the latter dendritic cell population accounted for ~15% of all lymphoid cells at day 4.

DISCUSSION

As previously reported for stroke[16] and other paradigms of sterile inflammation,[17] we observed a significant and early immigration of neutrophils into the ischemic brain accompanied by a massive influx of monocytes and macrophages. As our investigations started 24 hours after stroke, we cannot judge, which cell population in fact initiates the inflammatory cascade. However, there is accumulating evidence that neutrophils are the first wave of leukocytes that pave the way for the succeeding monocytes, which eventually differentiate into macrophages and dendritic cells.[18] Interestingly, we observed that the meninges covering the ischemic area seem to be the exclusive point of entry for the aforementioned first wave of leukocytes. Mast cells residing in the meninges have been discussed as important factor for the early influx of neutrophils,[19,20] which in turn attracted monocytes by releasing 'find me' and 'eat me' signals. This fundamental immunologic sequence is tightly controlled by negative feedback on the granulopoiesis via IL-23/IL-17.[21] Accordingly, we observed an almost complete decline of intracerebral and peripheral neutrophil counts to control levels 4 days after stroke. At this point, our results and those of others[16] are in contrast to findings reported by Gelderblom *et al*[22,23] who described a relatively late peak of neutrophil infiltration at day 3 after transient ischemia/reperfusion injury, primarily initiated by infiltrated $\gamma\delta$-T cells. It is possible that different stroke models differentially influence the meninges and their role as important gatekeepers for early neutrophil recruitment. Transient ischemia/reperfusion injury by means of the filament model typically produces an infarct core within the basal ganglia whereas cortical and meningeal damage is secondary. In contrast, the integrity of the meninges is *per se* compromised in stroke models using craniotomy, as we did in the present study. Finally, it is also possible that the inflammatory preactivation of hypertensive rats accelerates the kinetics of neutrophil infiltration. Discrepancies in the neutrophil turnover are translationally relevant, as it is generally believed that neutrophils have a deteriorating impact during poststroke inflammation.[24] Finally, it is presumed that neutrophils orchestrate the later infiltration of myeloid cells which for their part significantly influence the outcome after ischemic tissue damage.[4,17]

The phenotypic differentiation of the mononuclear myeloid cell family is challenging and yet not standardized.[18] To approach the problem of myeloid identity among infiltrating leukocytes, we discriminated the CD11b+ cells into CD45 low microglia,[16] CD45

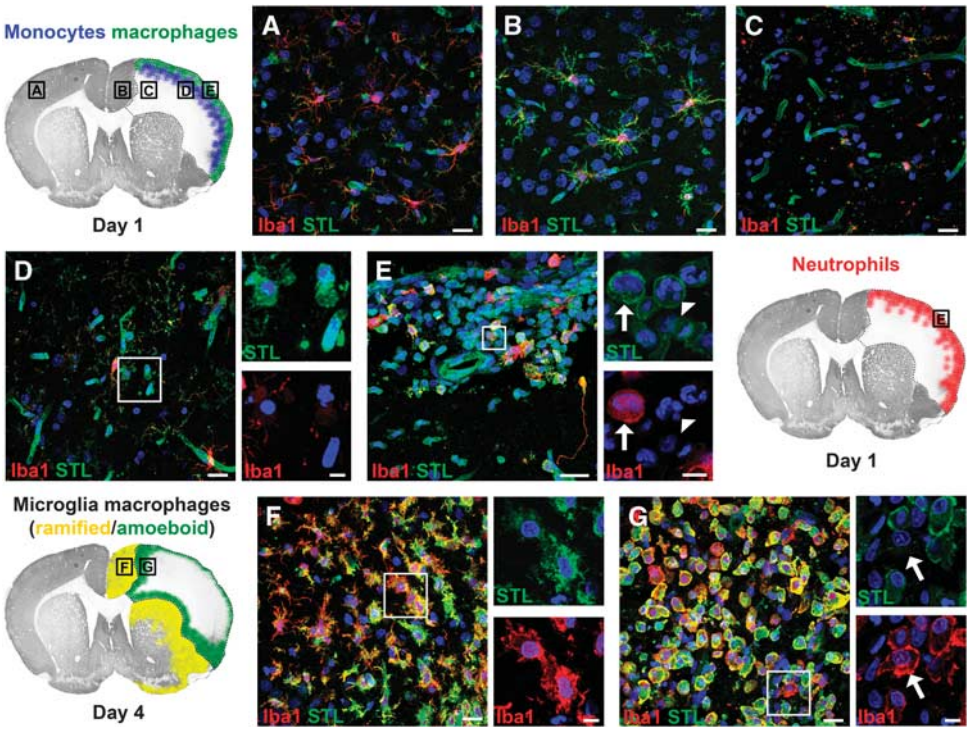

Figure 5. Spatial distribution of myeloid cell subpopulations. The schemes show the distribution pattern of different myeloid subpopulations and the localization of the respective magnifications. Figure **A** displays a representative magnification from the contralateral cortex, showing a STL + /Iba1 + microglia with thin, elongated processes. The cortical infarct border (**B**), however, is characterized by STL + /Iba1 + microglia with hypertrophied cell bodies and processes. (**C**) In the ischemic lesion, the STL + endothelium is still visible, whereas virtually all microglial cells disappeared. (**D**) STL + /Iba1 − monocytes were observed in the vicinity and remote from vessels in a region subjacent to the meninges. In contrast, we found STL + /Iba1 + macrophages/microglia (arrow) and STL + /Iba1 − /segmented nucleus neutrophils (arrowhead) adjacent to the part of the meninges covering the ischemic lesion (**E**). At day 4, the ischemic lesion is dominated by macrophages/microglia. Along the entire infarct border zone, we found numerous STL + /Iba1 + microglia with short, thick processes. In comparison with day 1 (**B**; the same region), we found a pronounced increase in the number of microglia, partially with a disruption of individual cellular domains (**F**). In the direction of the lesion, the STL + /Iba1 + cells adopt more and more a round (ameboid) phenotype, and could thus not reliably be distinguished into activated microglia or macrophages. Among the dense infiltrate of round STL + /Iba1 + cells, we could observe few Iba1 − /non-segmented nucleus monocytes (**G**; arrow). Scale bars, large images, 20 μm; small images, 5 μm.

high MHCII − monocytes,[25] which were also Iba1 −,[26] CD45 high CD11c + /CD80 + /CD86 + myeloid DCs and the remaining macrophage population (CD45 high MHCII + /Iba1 + /CD11c −). Applying these criteria, we observed distinctive kinetics of myeloid cell infiltration. Both at day 1 and 4 after the onset of stroke, we found a significant influx of CD45 high myeloid cells into the ischemic brain when compared with control or sham conditions, whereas the total amount of microglia was unchanged. At day 1, the myeloid infiltrate consisted of ~29% macrophages, 64% monocytes, and 8% myeloid dendritic cells. These early infiltrating myeloid cells most likely emanate from CCR2 + peripheral blood monocytes, which have been described to rapidly enter injured tissue, differentiate into macrophages or dendritic cells, and resume important functions by controlling clearance, mounting of T-cell responses, and repairing the neurovascular unit.[4,18] At day 4, we found the amount of monocytes and myeloid dendritic cells decreased to normal levels and that of macrophages almost halved. In contrast, we detected a clear increase of microglia within the entire infarct border zone. There are two possible explanations for this observation: first, microglia counts could increase as a consequence of local proliferation. Indeed, it has been shown that proliferating microglia has a protective role during postischemic inflammation, among others by releasing neurotrophic molecules.[27] The potential proliferation of microglia in our model is especially affirmed by the finding that after 24 hours, microglia counts in the MCAO group did not significantly differ from the sham-operated group even though stroke caused a 20% loss of microglial cells in the ischemic hemisphere due to pan-necrosis. A second explanation is that some of the infiltrated monocytes may have differentiated into microglia, as seen after blood–brain barrier disruption.[28] Even though this hypothesis requires confirmation in further radiation chimera studies, it would explain the simultaneous decline of infiltrated monocytes, a finding that is in contrast to what is known from other paradigms of sterile postischemic inflammation.[17]

We found that in naïve SH rats ~90% of the resident microglia express the CD4 receptor. Generally, microglial CD4 expression is an established phenomenon during activation and inflammation, but has been described on much lower levels under steady-state conditions.[29] It is possible that the high amount of CD4 + microglia in SH rats reflects a widespread activation of these cells in response to arterial hypertension, injured microvessels, and a perturbed blood–brain barrier.[10] Shortly after stroke, we found a transient increase of the proportion of CD4 − microglia to ~20%. The cause and importance of this observation are not completely understood yet. Considering the specific role of CD4 + microglia during the recovery phase of experimental autoimmune encephalomyelitis[29] and the low excitability of SH rat microglia in response to lipopolysaccharide injection and stroke,[30] one might speculate about a potential link between a hypertensive phenotype and the endogenous potential to clear sterile inflammation after stroke. Interestingly, it has been described

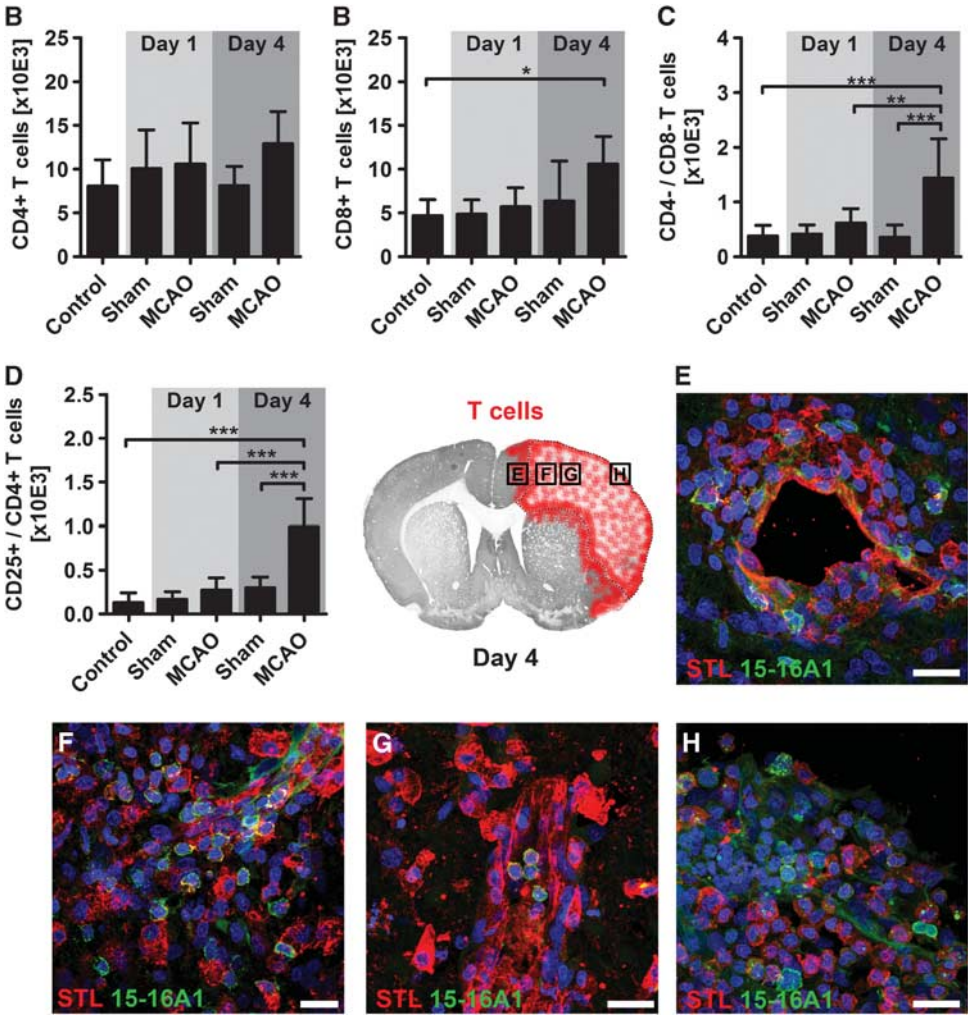

Figure 6. Characterization of brain-infiltrating T cells after stroke. (**A**) Quantification of total brain-infiltrating CD4+ T helper cells did not reveal any significant shifts because of sham surgery or middle cerebral artery occlusion (MCAO), although 4 days after stroke a tendency toward an increase was observed. (**B**) In contrast, CD8+ cytotoxic T cells showed a significant increase at day 4 when compared with the naïve control. Finally, a significant increase of CD4−/CD8− cells (**C**) and of CD25+/CD4+ cells (**D**) was observed at day 4 upon the onset of stroke. At this time point, T cells were found around periinfarct vessels (**E**), throughout the entire ischemic lesion with and without vicinity to vessels (**F** and **G**) and within the part of the meninges covering the ischemic lesion (**H**). $^{*}P<0.05$; $^{**}P<0.01$; $^{***}P<0.001$ by one-way analysis of variance for $n=5$ to 8 animals per group. Scale bars, 20 μm.

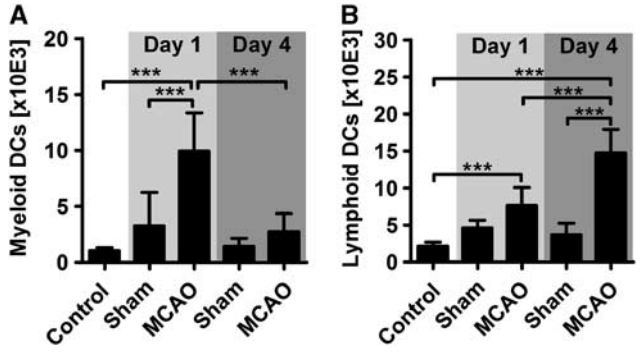

Figure 7. Characterization of brain-infiltrating dendritic cells after stroke. (**A**) Numbers of myeloid dendritic cells (DC) were significantly increased within brain infiltrates at day 1 after stroke, but not at day 4. (**B**) Lymphoid CD4+ DC increased successively from day 1 to day 4. $^{***}P<0.001$ by one-way analysis of variance for $n=5$ to 8 animals per group. MCAO, middle cerebral artery occlusion.

that the myeloid expression of CD4 is evident in rats and humans but not in mice,[31] indicating an important immunologic difference between the common stroke models.

The role of T cells in stroke immunology was first emphasized by the use of lymphocyte-deficient mice. The absence of both CD4+ and CD8+ T cells but not of B cells protects mice from ischemia/reperfusion injury at an early time point.[32] Later it was shown that early T-cell effects are not mediated by adaptive immune mechanisms but rather represent a consequence of endothelial dysfunction and subsequently decreased cerebral perfusion.[3] T cell–endothelium interactions could not be investigated in our model because of technical obligations (perfusion of cerebral vasculature). However, we observed a significant infiltration of cytotoxic T cells, but not of T helper cells at day 4 after stroke. This finding is in line with a previous histologic study of stroke, also showing that predominantly cytotoxic T cells infiltrate the ischemic brain tissue.[33] In our study, the CD4/CD8 ratio was unchanged in the peripheral blood throughout the experiment indicating that this 'skewed' infiltration is likely a specific

phenomenon. During the investigated stage of postischemic inflammation, cytotoxic T cells may harm viable brain tissue by releasing toxic substances such as granzyme-b.[34] Acute and predominantly adverse effects have also been attributed to $\gamma\delta$-T cells by mediating an increased neutrophil recruitment.[2,22] Along with invariant nature killer T cells, $\gamma\delta$-T cells are likely the major part of the CD3+ CD4−/CD8− population that was found to be increased at day 4 in our study. However, detailed analyses of T-cell subpopulations require specialized antibody panels and clearly go beyond the scope of this study.

Beyond the abovementioned acute effects of T cells, it is currently unknown whether T cells mediate antigen-dependent effects after cerebral stroke. Indeed, several lines of evidence argue in this direction.[35] It is assumed that the presentation of brain antigens within the peripheral lymphatic tissue is one prerequisite for the initiation and specific regulation of T-cell responses.[36] Brain antigens could reach the secondary lymphatic tissues passively, after being released through the disrupted blood–brain barrier, or actively by cellular transport. Thus, it was shown in rodents that circulating inflammatory monocytes and descendent monocyte-derived dendritic cells have the ability to enter the injured brain and to subsequently leave it toward the cervical lymph nodes via the cribriform plate.[37] Information on the presence of dendritic cells in the ischemic brain tissue is hence important for studying and understanding potential postischemic adaptive autoimmune processes. However, it is difficult to interpret our findings pertaining to dendritic cells, as this cell family is complex whereas only few data are available on rat dendritic cell identification.[38] However, we could differentiate two putative dendritic cell populations that sequentially entered the ischemic hemisphere. CD11b+ myeloid dendritic cells peaked together with monocytes and macrophages at day 1 after stroke and decreased to normal levels until day 4. By contrast, a CD4+ lymphoid dendritic cell population continuously increased toward day 4. Interestingly, it has been shown in the experimental allergic encephalomyelitis model that CD4+ lymphoid DCs can suppress T-cell-driven autoimmunity,[39] indicating the existence of a hitherto undescribed regulatory cell population in poststroke inflammation.

The most frequently used endpoint in preclinical stroke research is the infarct volume. Postischemic inflammation has been implicated to cause a delayed (>24 hours) infarct growth,[2] thus suggesting not only a prolonged therapeutic time window for immunomodulating agents but also the availability of a determinable endpoint. By contrast, we did neither see a secondary increase of the edema-corrected ischemic lesion nor a loss of viable brain tissue within the first days after stroke.[13] Delayed infarct growth has been observed in models of transient MCAO in the majority of cases. It is assumed, however, that the hemodynamics of permanent MCAO reflect the situation in patient much better than transient mechanical occlusion with instantaneous restoration of the blood flow after a designated period of time.[40] Here, the interpretation of our findings is limited by the fact that the hypertensive state was not controlled because of insufficient and heterogeneous ischemic lesions in normotensive strains after permanent distal MCAO. Hence, we could not judge here whether the lack of secondary infarct growth is a consequence of the permanent stroke model or the prevalent hypertensive condition or of both. Future studies approaching this subject should focus on stroke models that are independent of the vascular status, such as photothrombotic stroke. Notwithstanding, our study suggests that postischemic sterile inflammation may not affect infarct volume under preclinical conditions resembling clinical stroke cases.

CONCLUSION

In conclusion, our work delineates the concerted infiltration of peripheral immune cells into the ischemic brain parenchyma of hypertensive rats. We thereby were able to specify the participating cell populations and the spatiotemporal dynamics of the inflammatory cascade in this model. At the first day after stroke primarily neutrophils, peripheral monocytes, and their descendants entered the brain along the meninges, whereas the situation at day 4 was dominated by microglia, macrophages, lymphatic dendritic cells, and T cells. Notably, postischemic sterile inflammation did not cause secondary tissue damage during the subacute stage of experimental stroke in SH rats. About parallels regarding the intrinsic vascular pathology of SH rats and stroke patients, this study established a basis for future investigations on the influence of hypertension on poststroke inflammation, and validates this important strain for further translational research.

DISCLOSURE/CONFLICT OF INTEREST

The authors declare no conflict of interest.

ACKNOWLEDGMENTS

The authors thank Dr Manja Kamprad for her expert advice and excellent technical support regarding flow cytometric acquisition and analysis. Further, we would like to thank Ute-Maria Riegelsberger for providing tissues for this study and technical support during the setup of animal experiments. Finally, we would like to thank Dr Gesa Weise who carefully reviewed the manuscript and initiated helpful discussions.

Author contributions: KM, DCW, JB, and TS conceived and coordinated the study. JS participated in the design of the study and helped to draft the manuscript. KM and CP carried out the experiments. KM assembled and interpreted the data and conducted the statistical analysis. KM, JB, and DCW wrote the manuscript. All authors read and approved the final manuscript.

REFERENCES

1 Iadecola C, Anrather J. The immunology of stroke: from mechanisms to translation. *Nat Med* 2011; **17**: 796–808.
2 Shichita T, Sugiyama Y, Ooboshi H, Sugimori H, Nakagawa R, Takada I *et al.* Pivotal role of cerebral interleukin-17-producing gamma deltaT cells in the delayed phase of ischemic brain injury. *Nat Med* 2009; **15**: 946–950.
3 Kleinschnitz C, Kraft P, Dreykluft A, Hagedorn I, Gobel K, Schuhmann MK *et al.* Regulatory T cells are strong promoters of acute ischemic stroke in mice by inducing dysfunction of the cerebral microvasculature. *Blood* 2013; **121**: 679–691.
4 Gliem M, Mausberg AK, Lee JI, Simiantonakis I, van RN, Hartung HP *et al.* Macrophages prevent hemorrhagic infarct transformation in murine stroke models. *Ann Neurol* 2012; **71**: 743–752.
5 Macrez R, Ali C, Toutirais O, Le MB, Defer G, Dirnagl U *et al.* Stroke and the immune system: from pathophysiology to new therapeutic strategies. *Lancet Neurol* 2011; **10**: 471–480.
6 Seok J, Warren HS, Cuenca AG, Mindrinos MN, Baker HV, Xu W *et al.* Genomic responses in mouse models poorly mimic human inflammatory diseases. *Proc Natl Acad Sci USA* 2013; **110**: 3507–3512.
7 Hayday AC, Peakman M. The habitual, diverse and surmountable obstacles to human immunology research. *Nat Immunol* 2008; **9**: 575–580.
8 Murray KN, Buggey HF, Denes A, Allan SM. Systemic immune activation shapes stroke outcome. *Mol Cell Neurosci* 2013; **53**: 14–25.
9 Pantoni L. Cerebral small vessel disease: from pathogenesis and clinical characteristics to therapeutic challenges. *Lancet Neurol* 2010; **9**: 689–701.
10 Harrison DG, Marvar PJ, Titze JM. Vascular inflammatory cells in hypertension. *Front Physiol* 2012; **3**: 128.
11 Zhou J, Ando H, Macova M, Dou J, Saavedra JM. Angiotensin II AT1 receptor blockade abolishes brain microvascular inflammation and heat shock protein responses in hypertensive rats. *J Cereb Blood Flow Metab* 2005; **25**: 878–886.
12 Zubcevic J, Waki H, Raizada MK, Paton JF. Autonomic-immune-vascular interaction: an emerging concept for neurogenic hypertension. *Hypertension* 2011; **57**: 1026–1033.
13 Riegelsberger UM, Deten A, Posel C, Zille M, Kranz A, Boltze J *et al.* Intravenous human umbilical cord blood transplantation for stroke: impact on infarct volume and caspase-3-dependent cell death in spontaneously hypertensive rats. *Exp Neurol* 2011; **227**: 218–223.
14 Chen J, Sanberg PR, Li Y, Wang L, Lu M, Willing AE *et al.* Intravenous administration of human umbilical cord blood reduces behavioral deficits after stroke in rats. *Stroke* 2001; **32**: 2682–2688.

15 Moller K, Stahl T, Boltze J, Wagner DC. Isolation of inflammatory cells from rat brain tissue after stroke. *Exp Transl Stroke Med* 2012; **4**: 20.
16 Clausen BH, Lambertsen KL, Babcock AA, Holm TH, gnaes-Hansen F, Finsen B. Interleukin-1beta and tumor necrosis factor-alpha are expressed by different subsets of microglia and macrophages after ischemic stroke in mice. *J Neuroinflammation* 2008; **5**: 46.
17 Nahrendorf M, Swirski FK, Aikawa E, Stangenberg L, Wurdinger T, Figueiredo JL *et al.* The healing myocardium sequentially mobilizes two monocyte subsets with divergent and complementary functions. *J Exp Med* 2007; **204**: 3037–3047.
18 Gordon S, Taylor PR. Monocyte and macrophage heterogeneity. *Nat Rev Immunol* 2005; **5**: 953–964.
19 Christy AL, Walker ME, Hessner MJ, Brown MA. Mast cell activation and neutrophil recruitment promotes early and robust inflammation in the meninges in EAE. *J Autoimmun* 2013; **42**: 50–61.
20 Arac A, Grimbaldeston M, Nepomuceno A, Olayiwola O, Pereira MP, Nishiyama Y *et al.* 201 Meningeal mast cell-dependent exacerbation of brain injury after stroke in mice. *Neurosurgery* 2013; **60**(Suppl 1): 186–187.
21 Stark MA, Huo Y, Burcin TL, Morris MA, Olson TS, Ley K. Phagocytosis of apoptotic neutrophils regulates granulopoiesis via IL-23 and IL-17. *Immunity* 2005; **22**: 285–294.
22 Gelderblom M, Weymar A, Bernreuther C, Velden J, Arunachalam P, Steinbach K *et al.* Neutralization of the IL-17 axis diminishes neutrophil invasion and protects from ischemic stroke. *Blood* 2012; **120**: 3793–3802.
23 Gelderblom M, Leypoldt F, Steinbach K, Behrens D, Choe CU, Siler DA *et al.* Temporal and spatial dynamics of cerebral immune cell accumulation in stroke. *Stroke* 2009; **40**: 1849–1857.
24 Allen C, Thornton P, Denes A, McColl BW, Pierozynski A, Monestier M *et al.* Neutrophil cerebrovascular transmigration triggers rapid neurotoxicity through release of proteases associated with decondensed DNA. *J Immunol* 2012; **189**: 381–392.
25 Steiniger B, Stehling O, Scriba A, Grau V. Monocytes in the rat: phenotype and function during acute allograft rejection. *Immunol Rev* 2001; **184**: 38–44.
26 Ajami B, Bennett JL, Krieger C, McNagny KM, Rossi FM. Infiltrating monocytes trigger EAE progression, but do not contribute to the resident microglia pool. *Nat Neurosci* 2011; **14**: 1142–1149.
27 Lalancette-Hebert M, Gowing G, Simard A, Weng YC, Kriz J. Selective ablation of proliferating microglial cells exacerbates ischemic injury in the brain. *J Neurosci* 2007; **27**: 2596–2605.
28 Mildner A, Schmidt H, Nitsche M, Merkler D, Hanisch UK, Mack M *et al.* Microglia in the adult brain arise from Ly-6ChiCCR2+ monocytes only under defined host conditions. *Nat Neurosci* 2007; **10**: 1544–1553.
29 Almolda B, Costa M, Montoya M, Gonzalez B, Castellano B. CD4 microglial expression correlates with spontaneous clinical improvement in the acute Lewis rat EAE model. *J Neuroimmunol* 2009; **209**: 65–80.
30 De GD, Stoop W, Zgavc T, Sarre S, Michotte Y, De KJ *et al.* Spontaneously hypertensive rats display reduced microglial activation in response to ischemic stroke and lipopolysaccharide. *J Neuroinflammation* 2012; **9**: 114.
31 Gibbings D, Befus AD. CD4 and CD8: an inside-out coreceptor model for innate immune cells. *J Leukoc Biol* 2009; **86**: 251–259.
32 Yilmaz G, Arumugam TV, Stokes KY, Granger DN. Role of T lymphocytes and interferon-gamma in ischemic stroke. *Circulation* 2006; **113**: 2105–2112.
33 Schroeter M, Jander S, Witte OW, Stoll G. Local immune responses in the rat cerebral cortex after middle cerebral artery occlusion. *J Neuroimmunol* 1994; **55**: 195–203.
34 Chaitanya GV, Schwaninger M, Alexander JS, Babu PP. Granzyme-b is involved in mediating post-ischemic neuronal death during focal cerebral ischemia in rat model. *Neuroscience* 2010; **165**: 1203–1216.
35 Gee JM, Kalil A, Thullbery M, Becker KJ. Induction of immunologic tolerance to myelin basic protein prevents central nervous system autoimmunity and improves outcome after stroke. *Stroke* 2008; **39**: 1575–1582.
36 Chamorro A, Meisel A, Planas AM, Urra X, van de BD, Veltkamp R. The immunology of acute stroke. *Nat Rev Neurol* 2012; **8**: 401–410.
37 Kaminski M, Bechmann I, Pohland M, Kiwit J, Nitsch R, Glumm J. Migration of monocytes after intracerebral injection at entorhinal cortex lesion site. *J Leukoc Biol* 2012; **92**: 31–39.
38 Ziegler-Heitbrock L, Ancuta P, Crowe S, Dalod M, Grau V, Hart DN *et al.* Nomenclature of monocytes and dendritic cells in blood. *Blood* 2010; **116**: e74–e80.
39 Legge KL, Gregg RK, Maldonado-Lopez R, Li L, Caprio JC, Moser M *et al.* On the role of dendritic cells in peripheral T cell tolerance and modulation of autoimmunity. *J Exp Med* 2002; **196**: 217–227.
40 Hossmann KA. The two pathophysiologies of focal brain ischemia: implications for translational stroke research. *J Cereb Blood Flow Metab* 2012; **32**: 1310–1316.

Supplementary Information accompanies the paper on the Journal of Cerebral Blood Flow & Metabolism website (http://www.nature.com/jcbfm)